PPM-1, a PP2Cα/β phosphatase, Regulates Axon Termination and Synapse Formation in *Caenorhabditis elegans*

Erik D. Tulgren, Scott T. Baker, Laramie Rapp, Allison M. Gurney, and Brock Grill[1]
Department of Pharmacology, University of Minnesota, Minneapolis, Minnesota 55455

ABSTRACT The PHR (**P**am/**H**ighwire/**R**PM-1) proteins are evolutionarily conserved ubiquitin ligases that regulate axon guidance and synapse formation in *Caenorhabditis elegans*, *Drosophila*, zebrafish, and mice. In *C. elegans*, RPM-1 (**R**egulator of **P**resynaptic **M**orphology-1) functions in synapse formation, axon guidance, axon termination, and postsynaptic GLR-1 trafficking. Acting as an E3 ubiquitin ligase, RPM-1 negatively regulates a MAP kinase pathway that includes: *dlk-1*, *mkk-4*, and the p38 MAPK, *pmk-3*. Here we provide evidence that *ppm-1*, a serine/threonine phosphatase homologous to human PP2Cα(PPM1A) and PP2Cβ(PPM1B) acts as a second negative regulatory mechanism to control the *dlk-1* pathway. We show that *ppm-1* functions through its phosphatase activity in a parallel genetic pathway with *glo-4* and *fsn-1* to regulate both synapse formation in the GABAergic motorneurons and axon termination in the mechanosensory neurons. Our transgenic analysis shows that *ppm-1* acts downstream of *rpm-1* to negatively regulate the DLK-1 pathway, with PPM-1 most likely acting at the level of *pmk-3*. Our study provides insight into the negative regulatory mechanisms that control the *dlk-1* pathway in neurons and demonstrates a new role for the PP2C/PPM phosphatases as regulators of neuronal development.

THE **P**am/**H**ighwire/**R**PM-1 (PHR) proteins are key regulators of neuronal development that function in synapse formation, axon termination and guidance, axon regeneration, and glutamate receptor trafficking (Schaefer *et al.* 2000; Wan *et al.* 2000; Zhen *et al.* 2000; Burgess *et al.* 2004; D'Souza *et al.* 2005; Lewcock *et al.* 2007; Li *et al.* 2008; Hammarlund *et al.* 2009; Park *et al.* 2009; Po *et al.* 2010). The PHR protein family includes: human Pam, mouse Phr1, zebrafish esrom/Phr1, *Drosophila* Highwire and *Caenorhabditis elegans* **R**egulator of **P**resynaptic **M**orphology (RPM)-1.

PHR proteins function through multiple downstream signaling pathways. In *C. elegans*, RPM-1 functions as part of an ubiquitin ligase complex that includes the F-box protein, **F**-box **Syn**aptic Protein (FSN)-1 (Liao *et al.* 2004). This complex negatively regulates a MAP kinase cascade that includes ***d**ual **l**eucine zipper-bearing **k**inase* (*dlk-1*), ***m**ap **k**inase **k**inase* (*mkk)-4*, ***p38 m**ap **k**inase* (*pmk*)*-3*, ***m**ap kinase **a**ctivated protein **k**inase* (*mak*)*-2*, and the transcription factor *cebp-1* (Nakata *et al.* 2005; Yan *et al.* 2009). *Drosophila* Highwire and mouse Phr1 negatively regulate the ortholog of DLK-1 through a similar mechanism (Collins *et al.* 2006; Lewcock *et al.* 2007; Wu *et al.* 2007; Saiga *et al.* 2009; Tada *et al.* 2009). Phr1 also ubiquitinates and negatively regulates the tuberin sclerosis complex (Murthy *et al.* 2004; D'Souza *et al.* 2005; Han *et al.* 2008). RPM-1 positively regulates signaling through a Rab GTPase pathway by binding to **G**ut Granule **Lo**ss (GLO)-4 (Grill *et al.* 2007).

While RPM-1 negatively regulates the DLK-1 pathway, there are a number of reasons to suspect that the DLK-1 pathway may also be controlled by other negative regulatory mechanisms. First, overexpression of *dlk-1* causes more dramatic phenotypes than *rpm-1* loss of function (lf), including uncoordinated movement and small body size (Nakata *et al.* 2005; Abrams *et al.* 2008). Second, the *dlk-1* pathway consists of five signaling molecules providing numerous points where regulation might occur. Third,

doi: 10.1534/genetics.111.134791
Manuscript received May 9, 2011; accepted for publication September 23, 2011
Available freely online through the author-supported open access option.
[1]Corresponding author: Department of Pharmacology, 6-120 Jackson Hall, University of Minnesota, Twin Cities Campus, 321 Church St. SE, Minneapolis, MN 55455. E-mail: bgrill@umn.edu

ubiquitination is a relatively slow-acting mechanism to restrict DLK-1 signaling. The observation that UEV-3 is a possible positive regulator of PMK-3 (Trujillo *et al.* 2010) further supports the idea that multiple mechanisms may control the DLK-1 pathway.

There is a large body of evidence that MAP kinases are negatively regulated by phosphatases including MAP kinase-specific phosphatases, and broad-acting PP2C/PPM family phosphatases (Lu and Wang 2008; Shi 2009; Bermudez *et al.* 2010). While MAP kinases are known to function in neurons (Ji *et al.* 2009; Samuels *et al.* 2009), the negative regulatory phosphatases that control MAP kinase signaling in neurons remain relatively poorly understood.

Here we provide evidence that neuronal development is regulated by a PP2C/PPM family phosphatase from *C. elegans* that we call ***p**rotein **p**hosphatase **m**g^{2+}/mn^{2+} dependent (ppm)-1*. We have found that *ppm-1* acts through its phosphatase activity to regulate axon termination and synapse formation by acting in a parallel genetic pathway to *fsn-1* and *glo-4*. Loss of function in *ppm-1* is suppressed by loss of function in *pmk-3* (p38 MAPK), suggesting that *ppm-1* negatively regulates *pmk-3* activity. This finding is consistent with our observation that *ppm-1* functions downstream of *rpm-1*. Overall, our observations demonstrate that the DLK-1 pathway is negatively regulated by at least two mechanisms in neurons: the action of a Skp, Cullin, F-box (SCF) complex that includes RPM-1 and FSN-1 and the activity of a serine/threonine phosphatase, PPM-1.

Materials and Methods

Genetics

C. elegans strains were maintained as described (Brenner 1974). Alleles used in this study include: *rpm-1(ju44)*, *glo-1(zu391)*, *fsn-1(hp1)*, *ppm-1/tag-93(ok578)*, *ppm-1/tag-93(tm653)*, *dlk-1(ju476)*, *mkk-4(ju91)*, and *pmk-3 (ok169)*. All double mutants were constructed following standard procedures, and were confirmed by the associated phenotypes or by PCR genotyping. *glo-4*, *ppm-1* double mutants were constructed by recombination without using visible markers. Primers and PCR conditions are available upon request. *fsn-1*; *ok578/tm653* animals were constructed using *dpy-11* linked to *ok578*, and *unc-42* linked to *tm653*. Non-dpy, non-unc animals with the genotype *fsn-1*; *ok578*, *dpy-11/unc-42*, *tm653* were scored for *trans*-heterozygous analysis. The transgenic strains used in this study are: *muIs32*[P$_{mec-7}$GFP] (Ch'ng *et al.* 2003), *juIs1*[P$_{unc-25}$SNB-1::GFP] (Hallam and Jin 1998), *bggEx35* [wrm613bH10], *bggEx33* [P$_{rgef-1}$::ppm-1 (cDNA F25D1.1c)], *bggEx34*, *40*, and *41* [P$_{mec-7}$::ppm-1 (cDNA F25D1.1c)], *bggEX58*, *59*, *60*, *61*, and *62* [P$_{mec-7}$::ppm-1 (D246N) (cDNA F25D1.1c)], and *bggEx55*, *56 and 57* [P$_{ppm-1}$::GFP].

Transgene constructs

To construct cell-specific expression vectors of *ppm-1*, a *ppm-1* cDNA (corresponding to the coding sequence of F25D1.1c.1) was amplified by RT–PCR from *C. elegans* RNA and cloned into the pCR8-Topo gateway entry vector (Invitrogen) to create pBG-GY146. pBG-GY146 was recombined into destination vectors containing the *rgef-1* promoter, the *mec-7* promoter, or the *myo-3* promoter to generate pBG-GY153 (P$_{rgef-1}$*ppm-1*), pBG-GY163 (P$_{mec-7}$*ppm-1*), and pBG-GY116 (P$_{myo-3}$*ppm-1*). The D246N point mutant of PPM-1 was generated by site-directed mutagenesis to create pBG-GY200 (pCR8 TopoGY *ppm-1* (D246A). pBG-GY200 was recombined into destination vectors containing the *mec-7* promoter to generate pBG-GY202 (P$_{mec-7}$*ppm-1* (D246N)). The fosmid wrm613bH10 and pBA183 (P$_{myo-2}$mCherry) were gifts from David Greenstein (University of Minnesota) and Brian Ackley (University of Kansas), respectively.

Transgenic animals were generated as described previously (Mello *et al.* 1991). Plasmid DNA of interest was injected at 1–25 ng/μl along with P$_{ttx-3}$RFP (50 ng/μl) or (P$_{myo-2}$mCherry 1.5–2.5 ng/μl) and pBluescript (50 ng/μl). Initially all transgenic animals were generated on *ppm-1*$^{-/-}$ backgrounds. To create transgenic animals that were *fsn-1*; *ppm-1* double mutants, *fsn-1*; *ppm-1* mutants were heat shocked and males were mated to array positive *ppm-1* mutants. For DLK-1 overexpression experiments, P*rgef-1*::dlk-1 was amplified by long PCR using pBG-57 as a template and injected at 5–10 ng/μl. For rescue experiments with PPM-1, pBG-GY163 (P*mec-7*::ppm-1) or pBG-GY202 (P*mec-7*::ppm-1 (D246N) were coinjected at 2 ng/μl with P*rgef-1*::dlk-1. For analysis of PPM-1 subcellular distribution, pBG-GY208 (P*unc-25*::mCherry-PPM-1) was injected at 5 ng/μl into *ppm-1 (tm653)*; *juIs1* animals.

Axon termination and synapse formation analysis

Analysis was carried out using a Nikon epifluorescent microscope and a Q-imaging camera at ×40 magnification. Live animals were anesthetized using 1% (v/v) 1-phenoxy-2-propanol in M9 buffer. Axon termination defects were quantified by scoring 1–3 pools of worms consisting of 7–20 animals from three or more independent experiments for each genotype. The mean for a given phenotype was calculated and is shown in all histograms. All error bars represent the standard error of the mean. Statistical significance was calculated using an unpaired *t*-test. For synapse formation defects, data were averaged from 20–30 animals from a minimum of three independent experiments. The error bars represent the standard error of the mean, and statistical significance was determined using an unpaired *t*-test. Results were considered significant for axon termination defects or synapse formation defects if a P value of <0.05 was obtained. All analysis was done without blinding for genotypes.

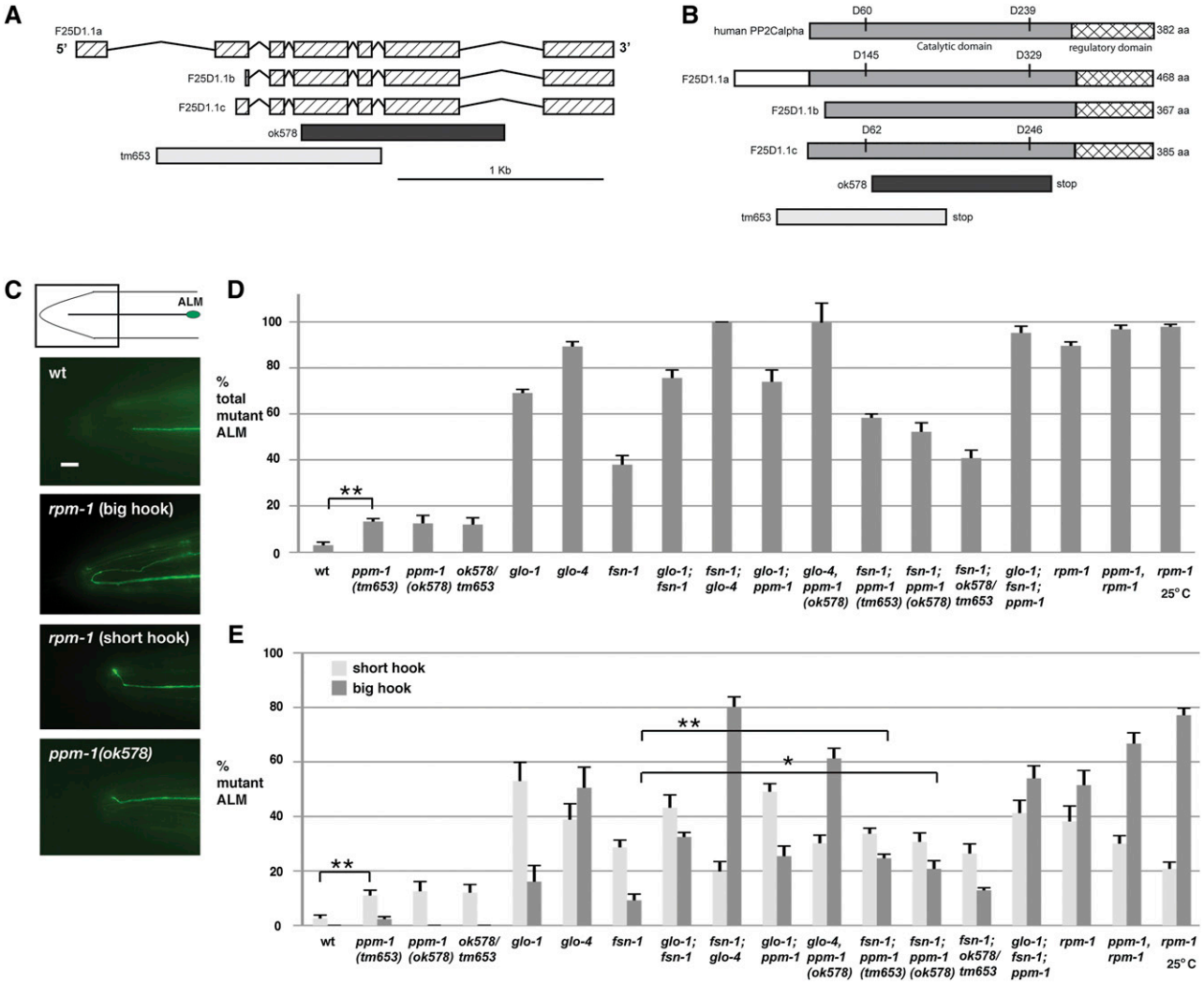

Figure 1 *ppm-1* regulates axon termination in the ALM neurons. (A) Schematic of the exons (hatched boxes) and introns of three open reading frames predicted for *ppm-1* by WormBase. The deletions caused by *ok578* and *tm653* are shown below. (B) Schematic of the human PP2Cα protein, and predicted PPM-1 proteins with the catalytic phosphatase domain (gray), and the regulatory domain (hatched design) highlighted. Shown below are segments of PPM-1 deleted by *ok578* and *tm653*. Mutagenesis studies on human PP2Cα showed that mutation of residue D60 and D239 led to 900- and 4000-fold decreases in phosphatase activity, respectively (Jackson *et al.* 2003). The corresponding conserved residues in PPM-1, D62, and D246 (F25D1.1c), are shown. (C) Axon termination defects in the ALM mechanosensory neuron were visualized using muIs32[P_{mec7}GFP] for wild type or the indicated mutant genotypes. Images correspond to the boxed region of the diagram. (D) Quantitation of the total axon termination defects in ALM neurons. (E) Quantitation of specific, short hook (white) or big hook (gray), axon termination defects in the ALM neurons of the indicated genotypes. Note that the percentage of ALM axons that are normal/wild type for each genotype is not shown. Analysis was performed on young adults grown at 23°, unless otherwise specified. Bar, 10 μm. Error bars represent the standard error of the mean. Significance was determined using an unpaired *t*-test, where *n* represents the number of independent counts of 10–30 worms for a given genotype. $*P < 0.05$, $**P < 0.01$.

Results

A PP2Cα/β phosphatase, PPM-1, regulates axon termination in the mechanosensory neurons of C. elegans

While the DLK-1 pathway is negatively regulated by RPM-1, several observations suggest that phosphatases of the PP2C/PPM family may also inhibit the DLK-1 pathway. Biochemical experiments *in vitro* and in mammalian cell culture have shown that PP2Cα and -β (also called PPM1A and -B) can dephosphorylate and negatively regulate MKKKs, MKKs, and MAPKs (Takekawa *et al.* 1998; Hanada *et al.* 2001). In yeast, the homologs of PP2Cα negatively regulate the activity of **H**igh-**o**smolarity **g**lycerol (Hog)1, the homolog of p38 MAPK (Maeda *et al.* 1994; Jacoby *et al.* 1997; Nguyen and Shiozaki 1999; Saito and Tatebayashi 2004). Further, PP2Cα functions in mammalian neurons to control calcium flux (Li *et al.* 2005), suggesting that PP2C phosphatases may have undiscovered roles in neuronal development.

The *C. elegans* genome contains a single gene, ***t**emporarily **a**ssigned **g**ene name (tag)-93* (*F25D1.1*), whose protein product is conserved with two PP2C phosphatases in humans, PP2Cα/PPM1A and PP2Cβ/PPM1B (49% identity

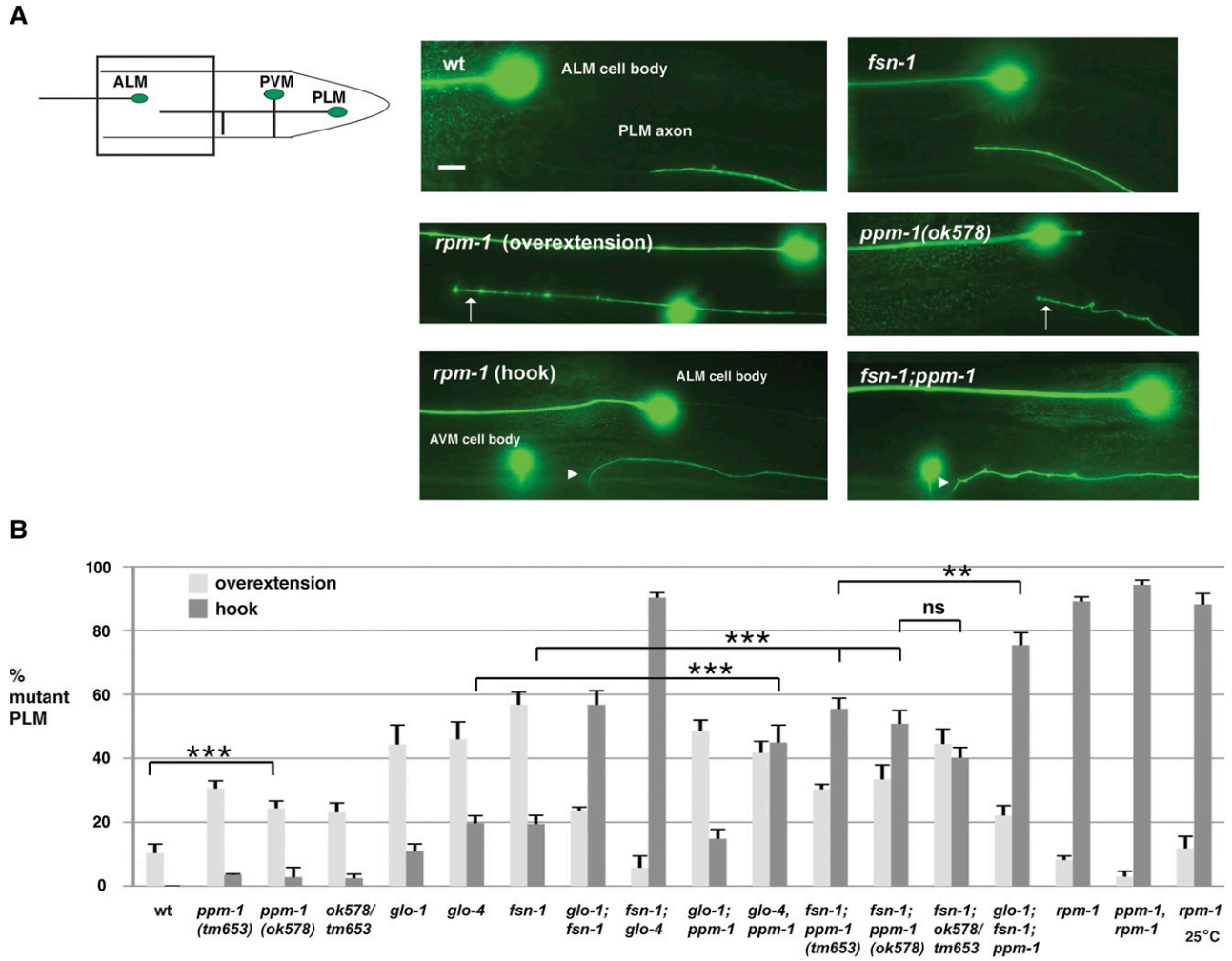

Figure 2 *ppm-1* regulates axon termination in the PLM neurons. (A) Axon termination defects in the PLM neurons were visualized using muIs32 [P_{mec7}GFP] for wild type or the indicated mutant genotypes. Images correspond to the boxed region of the diagram. Arrows mark overextension of the PLM axon beyond the ALM cell body, and arrowheads mark the more severe phenotype of overextension and hooking of the PLM axon. (B) Quantitation of the percentage of PLM neurons that only overextend (white) or overextend and hook (gray) for the indicated genotypes. Note that the percentage of PLM axons that are wild type for each genotype is not shown. Analysis was performed on young adults grown at 23°, unless otherwise specified. Bar, 10 μm. Error bars represent the standard error of the mean. Significance was determined using an unpaired *t*-test, where *n* represents the number of independent counts of 10–30 worms for a given genotype. ***$P < 0.001$; ns = not significant.

and 69% conservation with PPM1A; 54% identity and 72% conservation with PPM1B) (Stern *et al.* 2007) (Figure 1, A and B). PP2C/PPM phosphatases are single subunit enzymes that require magnesium/manganese for activity, and consist of a catalytic domain and a regulatory domain (Lu and Wang 2008; Shi 2009) (Figure 1B). On the basis of this homology, we have renamed *tag-93* as ***p**rotein **p**hosphatase **m**agnesium^{2+}/manganese^{2+} dependent (ppm)-1*.

There are three open reading frames of *ppm-1* that are predicted in the *C. elegans* genome (*F25D1.1a*, *F25D1.1b*, and *F25D1.1c*) (www.wormbase.org). One of these open reading frames, *F25D1.1c*, encodes a 385-amino-acid protein that has a conserved start site with mammalian PP2Cα/PPM1A (data not shown and Figure 1, A and B). Using RT–PCR, we confirmed the coding sequence of *F25D1.1c*, and we used this transcript as our frame of reference for analysis of two alleles of *ppm-1*: *ok578* and *tm653*. We sequenced the lesion in *ok578* and found that it deletes 984 bp and inserts two thymidine bases, which causes a frameshift and leads to loss of wild-type sequence after amino acid 69. Importantly, *ok578* deletes a residue (D246) that when mutated in mammalian PP2Cα/PPM1A results in a 4000-fold drop in phosphatase activity (Jackson *et al.* 2003) (Figure 1B). Sequencing of *tm653* confirmed it has a 1089-bp deletion in the *ppm-1* gene that deletes a portion of the promoter, the start codon, and the first 156 amino acids of PPM-1 including a key catalytic residue (Figure 1B). These observations show that *ok578* and *tm653* are molecular null alleles.

Defects in *rpm-1*(*lf*) mutants are due, in part, to excess signaling through the *dlk-1* pathway (Nakata *et al.* 2005; Grill *et al.* 2007). We hypothesized that *ppm-1*(*lf*) might also

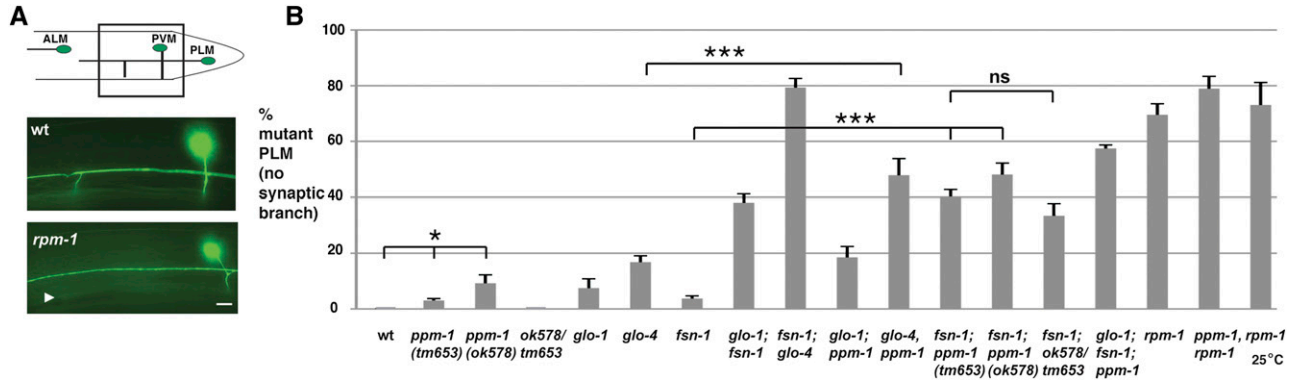

Figure 3 *ppm-1* regulates synaptic branch extension/stabilization in PLM neurons. (A) Defects in synaptic branch extension in the PLM neurons were visualized using muIs32[P_{mec7}GFP] in wild type or the indicated mutant genotypes. Images correspond to the boxed region of the diagram. Arrowhead highlights the absence of the synaptic branch. (B) Quantitation of the defects in synaptic branch extension in the PLM neurons for the indicated genotypes. Note that the percentage of PLM axons that are wild type for each genotype is not shown. Analysis was performed on young adults grown at 23°, unless otherwise specified. Bar, 10 μm. Error bars represent the standard error of the mean. Significance was determined using an unpaired *t*-test, where *n* represents the number of independent counts of 10–30 worms for a given genotype. $*P < 0.05$, $***P < 0.001$; ns, not significant.

increase signaling through the *dlk-1* pathway and result in phenotypes that are similar to *rpm-1*(*lf*) mutants. To test this hypothesis, we first analyzed the mechanosensory neurons of *ppm-1*(*lf*) mutants.

In wild-type animals, the two anterior lateral microtubule (ALM) mechanosensory neurons each have a single axon that terminates at a precise location (Figure 1C). In contrast, axon termination is defective in the ALM neurons of *rpm-1*(*lf*) mutants (Figure 1, C and D). *rpm-1*(*lf*) mutants display two types of ALM axon termination defects: less severe short hooks and more severe big hooks where the axon overextends and hooks toward the posterior of the animal (Figure 1, C and E). In *rpm-1*(*lf*) mutants, big hooks in the ALM are the predominant phenotype, and this phenotype is temperature sensitive for the *ju44* allele of *rpm-1* (Figure 1E). In *ppm-1(ok578)* and *ppm-1(tm653)* mutants, we observed small hook defects in the ALM neurons that occurred with low penetrance (Figure 1, C–E).

Previous studies showed that *rpm-1*(*lf*) mutants also have defects in the posterior lateral microtubule (PLM) neurons, which fall into two main phenotypic categories: (1) axon termination defects (Figure 2A) and (2) synaptic branch extension/stabilization defects (Figure 3A) (Schaefer *et al.* 2000; Grill *et al.* 2007). A given PLM neuron can display one or both of these phenotypes. In *rpm-1*(*lf*) mutants, a small percentage of PLM axons (8%) display a milder axon termination phenotype in which the PLM axon only overextends beyond the ALM cell body (Figure 2A, overextension). The majority of PLM neurons in *rpm-1*(*lf*) mutants (90%) display a more severe phenotype in which the PLM axon overextends beyond the ALM cell body and also hooks ventrally, which we will refer to as hooking for ease of discussion (Figure 2A, hook). Both the hooking and synaptic branch defects in *rpm-1*(*lf*) mutants are highly penetrant (Figures 2B and 3B). In *ppm-1(ok578)* mutants, we observed both axon termination phenotypes with a larger percentage of neurons showing the milder overextension phenotype and a small percentage of neurons showing the more severe hooking phenotype (Figure 2, A and B). Similar results were obtained for *ppm-1(tm653)* (Figure 2B). With regard to synaptic branch extension, *ppm-1*(*lf*) animals had defects in synaptic branch extension that were very low penetrance (Figure 3, A and B). These results show that *ppm-1* regulates axon termination in the mechanosensory neurons.

ppm-1 functions in parallel to *fsn-1* and *glo-4* to regulate axon termination

rpm-1 has two major downstream signaling activities that are known. *rpm-1* functions with *fsn-1* to negatively regulate the *dlk-1* pathway (Liao *et al.* 2004; Nakata *et al.* 2005) and binds to GLO-4 to positively regulate the *glo* pathway, which includes: *glo-4*, *glo-1* (a Rab GTPase), and *apm-3* (Grill *et al.* 2007). To determine whether *ppm-1* functions in either of these pathways or as part of an independent pathway, we constructed double mutants between *ppm-1* and *fsn-1*, *glo-4*, and *glo-1*. When total mutant neurons were analyzed, *fsn-1*; *ppm-1* double mutants had an additive phenotype in the ALM neurons (Figure 1B). However, an enhanced penetrance of big hooks was observed in *fsn-1*; *ppm-1* double mutants compared to single mutants (Figure 1E). Both *ppm-1(ok578)* and *ppm-1(tm653)* had similar enhancer effects with *fsn-1*(*lf*) (Figure 1E). While the level of big hooks was mildly increased in both *glo-4*, *ppm-1* and *glo-1*; *ppm-1* double mutants, these differences were not statistically significant, demonstrating that *ppm-1* does not enhance the *glo* pathway in the ALM neurons (Figure 1E).

With regard to the PLM neurons, *fsn-1*; *ppm-1* double mutants had an enhanced percentage of neurons that show the hooking phenotype (Figure 2). The penetrance of synaptic branch defects was also strongly enhanced in *fsn-1*; *ppm-1* double mutants (Figure 3B). Both alleles of *ppm-1* (*ok578* or *tm653*) gave similar levels of enhancement with *fsn-1*. The axon termination (hooking) and synaptic branch extension defects in the PLM neurons of *glo-4*, *ppm-1* double

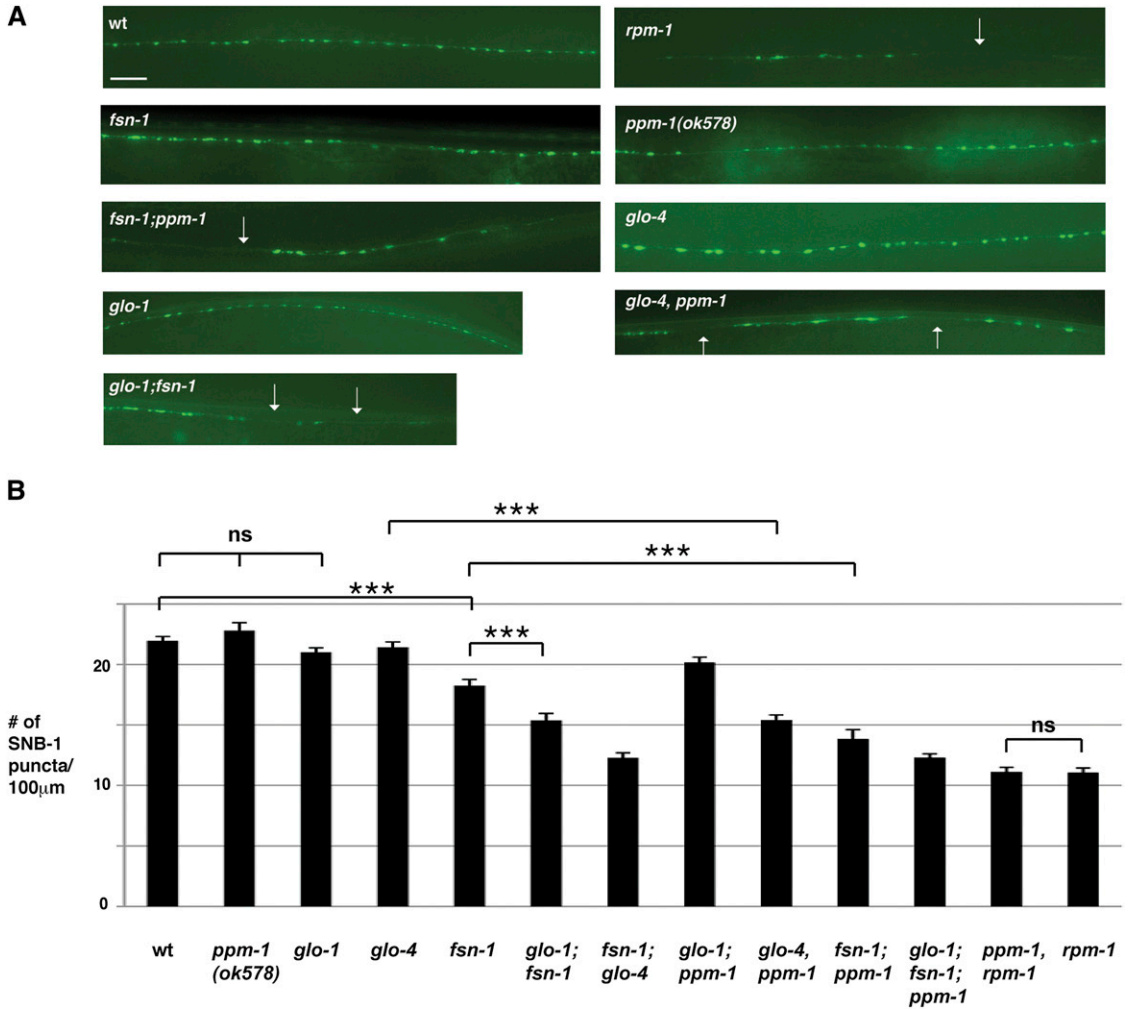

Figure 4 *ppm-1* regulates synapse formation in GABAergic motor neurons. (A) Presynaptic terminals of DD neurons were visualized using *juIs1*[P_{unc-25} SNB-1::GFP] in wild type or mutant genotypes. Arrows highlight the gaps between presynaptic puncta in the dorsal cord. (B) Quantitation of the average number of SNB-1::GFP puncta per 100 μm of dorsal cord. Analysis was performed on young adults grown at 25°. Bar, 10 μm. Significance was determined using a Student's *t*-test, and error bars represent the standard error of the mean. ***$P < 0.001$; ns, not significant.

mutants were also enhanced (Figures 2B and 3B). In contrast, axon termination and branch extension defects in the PLM neurons of *glo-1*; *ppm-1* double mutants and *glo-1*; *fsn-1*; *ppm-1* triple mutants were increased, but not enhanced (Figures 2B and 3B). *fsn-1*; *glo-4*, *ppm-1* triple mutants were not analyzed as *fsn-1*; *glo-4* double mutants have maximal phenotypes (Figures 2B and 3B) (Grill *et al.* 2007).

To test whether the two alleles of *ppm-1* analyzed were null mutants, we performed *trans*-heterozygous analysis. With regard to the PLM neurons, *fsn-1*; *ok578/tm653* mutants showed enhanced penetrance of defects in axon termination and synaptic branch extension (Figures 2B and 3B) that were not significantly different from *fsn-1*; *ppm-1(ok578)* and *fsn-1*; *ppm-1(tm653)* double mutants. These results are consistent with *ok578* and *tm653* acting as null alleles of *ppm-1* in the PLM neurons. In the ALM neurons, *fsn-1*; *ok578/tm653* had an increased percentage of neurons showing big hooks compared to *fsn-1* single mutants; however, levels were not increased to the same extent as *fsn-1*; *ppm-1(ok578)* and *fsn-1*; *ppm-1(tm653)*. Thus, in the ALM neurons the genes used as visible markers to generate *fsn-1*; *ok578/tm653* animals (*dpy-11* and *unc-42*) may affect *ppm-1*, or the ALM neurons may be less sensitive to *ppm-1* loss of function.

Overall, our data are consistent with a model in which *ppm-1* functions in a parallel pathway to *fsn-1* and *glo-4* to regulate axon termination and synaptic branch extension/stabilization in the PLM mechanosensory neurons.

ppm-1 regulates synapse formation in GABAergic motor neurons

Previous studies have shown that *rpm-1* regulates synapse formation in the motor neurons (Zhen *et al.* 2000; Nakata *et al.* 2005). The presynaptic terminals formed by the GABAergic dorsal D type (DD) motor neurons can be visualized with **Syn**apto**b**revin (SNB)-1 fused to GFP (GFP::SNB-1). In wild-type animals, GFP::SNB-1 puncta of the DD neurons are evenly distributed along the dorsal nerve

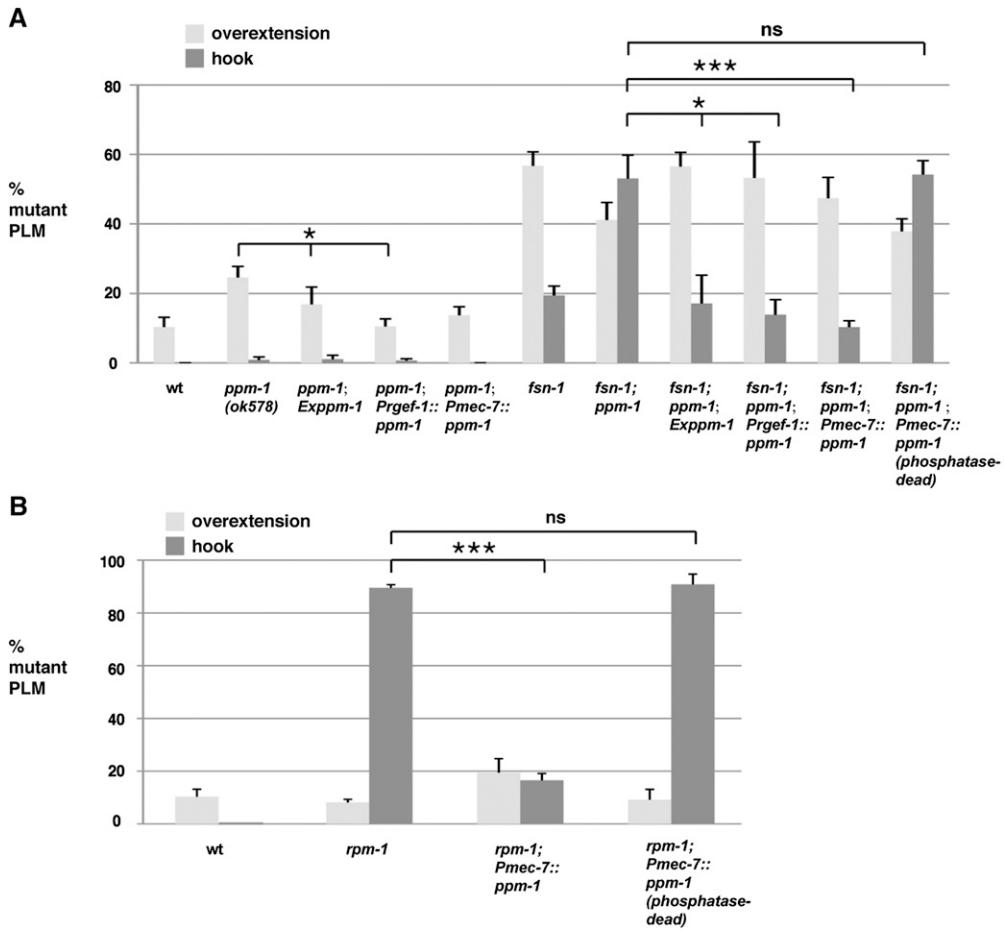

Figure 5 Transgenic expression of *ppm-1* in the mechanosensory neurons rescues *ppm-1*(*lf*) defects in axon termination. (A) Recue of axon termination defects in the PLM neurons of *ppm-1* or *fsn-1*; *ppm-1* mutants by transgenic expression of PPM-1 using the indicated promoters. The percentage of PLM axons that overextend only (white) or overextend and hook (gray) are shown. The percentage of PLM neurons with normal axon termination is not shown. For all transgenes, the data shown are from two to three transgenic lines, except for the fosmid wrm613bH10 (*Exppm-1*) in which only one transgenic line was analyzed. (B) Axon termination defects in *rpm-1*(*lf*) mutants are partially rescued by transgenic expression of PPM-1, but not by transgenic expression of phosphatase-dead PPM-1 (D246N). The data shown are from two to three transgenic lines for each genotype. Analysis was performed on young adults grown at 23°. Error bars represent the standard error of the mean. Significance was determined using an unpaired *t*-test, where *n* represents the number of independent counts of 10–30 worms for a given genotype. $*P < 0.05$, $***P < 0.001$.

cord (Figure 4A). In contrast, *rpm-1*(*lf*) mutants have disorganized GFP::SNB-1 puncta with gaps and aggregation (Figure 4A). While *ppm-1*(*lf*) animals are normal, *fsn-1*; *ppm-1* and *glo-4*, *ppm-1* double mutants are enhanced with significant disorganization of GFP::SNB-1 puncta (Figure 4A) and reduced numbers of SNB-1::GFP puncta (Figure 4B). *glo-1*; *ppm-1* double mutants had reduced numbers of SNB-1::GFP puncta, but defects were too mild to constitute enhancement (Figure 4B, $P < 0.05$). We also observed that *ppm-1*, *rpm-1* double mutants have similar defects as those in *rpm-1*(*lf*) mutants. Importantly, synapse formation defects in *rpm-1*(*lf*) mutants are not saturated, as defects become significantly worse in *rpm-1*; *syd-2* double mutants (Liao *et al.* 2004). Therefore, our observations are consistent with *ppm-1* regulating synapse formation by functioning in the same genetic pathway as *rpm-1*, and a parallel genetic pathway to *fsn-1* and *glo-4*.

ppm-1 functions in mechanosensory neurons downstream of rpm-1

rpm-1 and its downstream signaling molecules, *glo-4* and *glo-1*, act cell autonomously in mechanosensory neurons (Schaefer *et al.* 2000; Grill *et al.* 2007). To determine whether *ppm-1* functions cell autonomously, we performed transgenic rescue experiments in which *ppm-1* expression was driven by different promoters. Transgenic expression of *ppm-1* using either a fosmid (native *ppm-1* promoter), P*rgef-1* (a pan-neuronal promoter), or P*mec-7* (a mechanosensory neuron promoter) rescued PLM axon termination defects in both *ppm-1* single mutants and *fsn-1*; *ppm-1* double mutants (Figure 5A). Previous studies identified a single point mutation (D239N) that results in a 4000-fold decrease in phosphatase activity in human PP2Cα (Jackson *et al.* 2003) (Figure 1A). *ppm-1* that is mutated at the corresponding residue (D246N), and presumably catalytically inactive, did not rescue the enhanced axon termination defects in *fsn-1*; *ppm-1* double mutants (Figure 5A). These results demonstrate that *ppm-1* regulates axon termination through its phosphatase activity, and that the lesion in *ok578* causes the enhanced penetrance of axon termination defects observed in *ppm-1*; *fsn-1* double mutants.

Our genetic analysis described earlier indicates that *ppm-1* functions in the same genetic pathway as *rpm-1*. To determine whether *ppm-1* functions up or downstream of *rpm-1*, we generated transgenic animals that overexpress PPM-1 in the mechanosensory neurons of *rpm-1*(*lf*) mutants. Overexpression of PPM-1 strongly, but partially, reduced the axon termination defects in *rpm-1*(*lf*) mutants (Figure 5B). In contrast, phosphatase-dead PPM-1 did not rescue axon termination defects in *rpm-1*(*lf*) mutants

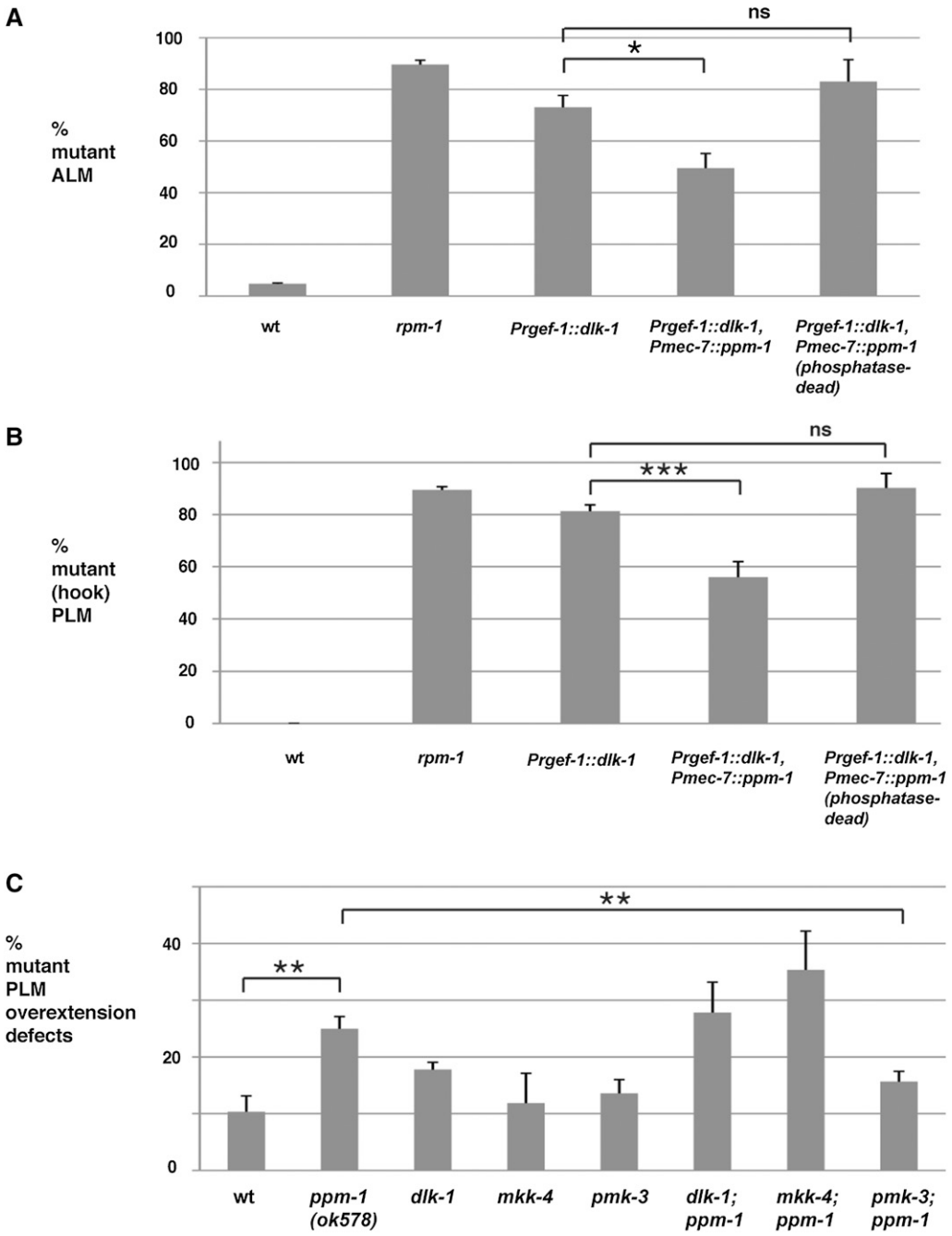

Figure 6 *ppm-1* negatively regulates the *dlk-1* pathway. Transgenic expression of DLK-1 causes axon termination defects in (A) ALM neurons and (B) PLM neurons, which is suppressed by coexpression of PPM-1, but not phosphatase-dead PPM-1 (D246N). The data shown are pooled from three or more transgenic lines, except the data for phosphatase-dead PPM-1, which are from a single transgenic line. The percentage of PLM axons that hook are shown. The percentage of PLM neurons that overextend or are wild type is not shown. (C) Analysis of suppression of *ppm-1* mutant phenotypes by loss of function in *dlk-1*, *mkk-4*, and *pmk-3*. Quantitation of axon termination defects (overextension only) is shown in the indicated mutant genotypes. Note that only *pmk-3*$^{-/-}$; *ppm-1*$^{-/-}$ mutant animals show a significant suppression of defects in axon termination. Analysis was performed on young adults grown at 23°. Error bars represent the standard error of the mean. Significance was determined using an unpaired *t*-test, where *n* represents the number of independent counts of 10–30 worms for a given genotype. *$P < 0.05$, **$P < 0.005$, ***$P < 0.001$.

(Figure 5B). These results are consistent with *ppm-1* functioning as a phosphatase that acts downstream of *rpm-1*.

ppm-1 negatively regulates the DLK-1 pathway

Previous studies have shown that the orthologs of PPM-1 can act at the level of MKKK, MKK, or MAPK to negatively regulate a kinase cascade (Takekawa *et al.* 1998; Hanada *et al.* 2001). These observations suggested that phenotypes in *ppm-1*(*lf*) mutants might be due to excess activation of *dlk-1*, *mkk-4*, and/or *pmk-3*. To address this question, we employed two experimental strategies. First, we used a transgenic approach to test whether *ppm-1* negatively regulates the DLK-1 pathway. Overexpression of DLK-1 resulted in similar severity and penetrance of phenotypes as those seen in *rpm-1*(*lf*) mutants including axon termination defects in the ALM (Figure 6A) and PLM neurons (Figure 6B), and defects in synaptic branch extension in the PLM neurons (data not shown). Coexpression of PPM-1, but not phosphatase-dead PPM-1, partially rescued the defects caused by overexpression of DLK-1 (Figure 6, A and B). This observation suggests that PPM-1 acts as a phosphatase to negatively regulate the DLK-1 pathway.

Next, we used a genetic approach to determine which kinase in the DLK-1 pathway might be a target of PPM-1's

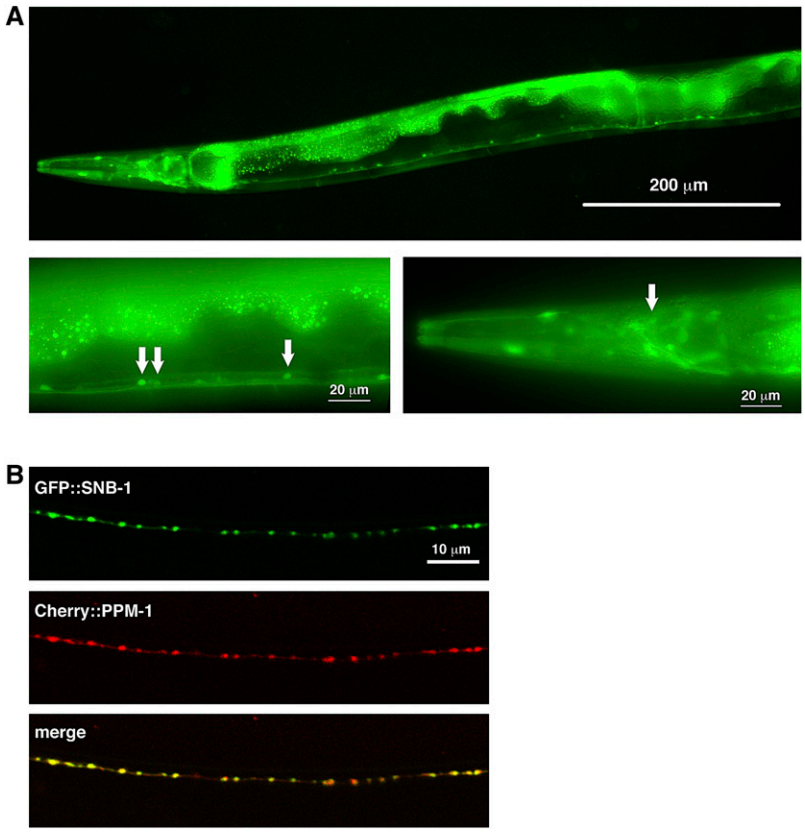

Figure 7 PPM-1 is expressed in neurons and localizes to presynaptic terminals. (A) Transgenic worms that use the 3.7-kb promoter of *ppm-1* (*F25D1.1*) to express GFP were analyzed by epifluorescent microscopy. GFP is expressed broadly by the *ppm-1* promoter (upper image), and is present in neurons of the ventral cord (arrows, lower left image), and the nerve ring (arrow, lower right image). (B) Confocal microscopy was used to analyze transgenic worms that express mCherry::PPM-1 (red) and GFP::SNB-1 (green) specifically in the GABAergic motor neurons using the *unc-25* promoter. mCherry::PPM-1 colocalizes with GFP::SNB-1 at presynaptic terminals in the dorsal nerve cord.

phosphatase activity. To do so, we constructed double mutants of *ppm-1* with *dlk-1*, *mkk-4*, or *pmk-3*. Axon termination defects (overextension) in the PLM neurons were analyzed for double mutants and compared to *ppm-1*(*lf*) single mutants. Defects in axon termination were not rescued in *dlk-1*; *ppm-1* and *mkk-4*; *ppm-1* double mutants (Figure 6C). In contrast, axon termination defects in *pmk-3*; *ppm-1* double mutants were significantly reduced compared to *ppm-1*(*lf*) single mutants (Figure 6C). These observations are consistent with excess *pmk-3* function leading to axon termination defects in *ppm-1*(*lf*) mutants.

PPM-1 localizes to the presynaptic terminals of motor neurons

Given that *ppm-1* functions in neurons, we wanted to test whether it is expressed in neurons. To address this question, we generated transgenic animals in which the 3.7-kb promoter of *ppm-1* drives expression of GFP. Pppm-1GFP is expressed in neurons of the nerve ring and motor neurons of the ventral nerve cord (Figure 7A). Since *ppm-1* is expressed in motor neurons, we used a transgenic approach to study the subcellular distribution of PPM-1 in the GABAergic DD and VD motor neurons. We generated transgenic animals that express a fusion protein of mCherry and PPM-1, and a fusion protein of GFP and SNB-1, a synaptic vesicle membrane protein. SNB-1::GFP localizes to presynaptic puncta in the dorsal cord where the DD neurons innervate muscle (Figure 7B). While mCherry::PPM-1 was not always punctate, mCherry::PPM-1 puncta were observed in the dorsal cord and colocalized with GFP::SNB-1 (Figure 7B). These results demonstrate that PPM-1 can localize to the presynaptic terminals of GABAergic motor neurons.

Discussion

RPM-1 functions as part of an E3 ubiquitin ligase/SCF complex that includes FSN-1. This complex ubiquitinates and destroys DLK-1 to negatively regulate a MAP kinase pathway (Nakata *et al.* 2005). RPM-1 is part of a conserved protein family called PHR proteins, and PHR proteins in flies and mice also function as part of SCF complexes to regulate synapse formation and neuronal development (Burgess *et al.* 2004; Collins *et al.* 2006; Lewcock *et al.* 2007; Wu *et al.* 2007; Saiga *et al.* 2009; Tada *et al.* 2009). Thus, negative regulation of the DLK-1/Dlk pathway represents an essential, evolutionarily conserved function of the PHR proteins. While PHR proteins represent one mechanism for negatively regulating the DLK-1 pathway, it remains uncertain if other, complementary mechanisms also restrain the activity of this pathway. Here we provide evidence of a conserved PP2Cα/β phosphatase, PPM-1, that also negatively regulates the DLK-1 pathway.

Our analysis shows that loss of function in *ppm-1* results in relatively mild phenotypes compared to *rpm-1*, and that *ppm-1*(*lf*) enhances *fsn-1* and *glo-4*(*lf*). This finding explains why *ppm-1* mutants were not isolated in previous genetic

screens for mutants with defective axon termination or synapse formation. Our observations are consistent with *ppm-1* functioning in a genetic pathway that is parallel to both *fsn-1* and *glo-4*.

With regard to axon termination in the PLM neurons, and synapse formation in the GABAergic motor neurons, we observed that *glo-4*, *ppm-1* double mutants were enhanced, and *glo-1*; *ppm-1* double mutants were not enhanced. This observation suggests that *glo-4* plays a greater role in axon termination and synapse formation than *glo-1*. This interpretation is consistent with our observations that *glo-4* has stronger enhancer effects than *glo-1* with *fsn-1* (Grill *et al.* 2007) (Figure 1–4). Presumably a certain level of reduced GLO pathway function is needed to enhance *ppm-1*(*lf*). While *glo-4*(*lf*) achieves this level of inactivation of the GLO pathway, *glo-1* does not. This model suggests that an unidentified small GTPase or signaling molecule, besides GLO-1, functions downstream of GLO-4. Presumably loss of function in both *glo-1* and this other molecule(s) is required to enhance *ppm-1*(*lf*).

Our observation that *ppm-1*(*lf*) does not enhance *rpm-1*(*lf*) demonstrates that *ppm-1* functions in the same genetic pathway as *rpm-1*. This is consistent with our transgenic experiments showing that *ppm-1* functions downstream of *rpm-1* to negatively regulate the DLK-1 pathway. Suppression of *ppm-1* axon termination defects by *pmk-3*(*lf*) suggests that PPM-1 may negatively regulate PMK-3 directly by dephosphorylation. Alternatively, PPM-1 may negatively regulate a positive regulator of PMK-3, such as UEV-3. Future biochemical experiments aimed at testing whether PPM-1 regulates the phosphorylation of PMK-3 should provide a definitive answer to this question.

It is not immediately clear to us why only *pmk-3*(*lf*) suppresses *ppm-1*(*lf*) defects. We anticipated that loss of function in any component of the DLK-1 pathway would prevent activation of this pathway and suppress phenotypes caused by *ppm-1*(*lf*). One explanation for our results is that kinases other than DLK-1 and MKK-4 also function upstream of PMK-3, and suppression only occurs with loss of function in the target of PPM-1, presumably PMK-3. Mixed Lineage Kinase (MLK)-1 was recently shown to function upstream of PMK-3 in the context of axon regeneration (Nix *et al*. 2011), and is a likely candidate as an alternative mechanism for activation of PMK-3 in the context of development.

Importantly, the *dlk-1* pathway is required not just in a developmental context, but also for axon regeneration in the mechanosensory neurons (Yan *et al.* 2009) and in the motor neurons of adult *C. elegans* (Hammarlund *et al.* 2009). Overexpression of *dlk-1*, or loss of function in *rpm-1* or *fsn-1*, leads to improved axon regeneration (Hammarlund *et al.* 2009). Our discovery that *ppm-1* is a negative regulator of the *dlk-1* pathway, similar to *rpm-1* and *fsn-1*, suggests that *ppm-1* may also function in axon regeneration. Given our finding that *ppm-1* enhances *fsn-1* with regard to defects in both axon termination and synapse formation, it is plausible that *fsn-1*; *ppm-1* double mutants may also show enhanced increases in axon regeneration. Future experiments aimed at addressing this possibility will be informative.

In summary, our study provides new insight into the molecular mechanisms of axon termination and synapse formation by showing that PPM-1 constitutes a new regulatory mechanism to control signaling through the DLK-1 pathway. Our study highlights the potential importance of the PP2C/PPM phosphatases in neuronal development. Addressing whether other members of the PP2C/PPM family function in axon termination and/or synapse formation remains an important goal for the future.

Acknowledgments

We thank David Greenstein, Lihsia Chen, and Yishi Jin for helpful discussions. We are grateful to the *Caenorhabditis elegans* Genetics Center and the *Caenorhabditis elegans* Knockout Consortium for providing strains and deletion mutants, respectively. Finally, we acknowledge Shane Turgeon's technical contributions. This work was supported by a grant from the Minnesota Medical Foundation and a grant-in-aid from the University of Minnesota.

Literature Cited

Abrams, B., B. Grill, X. Huang, and Y. Jin, 2008 Cellular and molecular determinants targeting the Caenorhabditis elegans PHR protein RPM-1 to perisynaptic regions. Dev. Dyn. 237: 630–639.

Bermudez, O., G. Pages, and C. Gimond, 2010 The dual-specificity MAP kinase phosphatases: critical roles in development and cancer. Am. J. Physiol. Cell Physiol. 299: C189–C202.

Brenner, S., 1974 The genetics of *Caenorhabditis elegans*. Genetics 77: 71–94.

Burgess, R. W., K. A. Peterson, M. J. Johnson, J. J. Roix, I. C. Welsh *et al.*, 2004 Evidence for a conserved function in synapse formation reveals Phr1 as a candidate gene for respiratory failure in newborn mice. Mol. Cell. Biol. 24: 1096–1105.

Ch'ng, Q., L. Williams, Y. S. Lie, M. Sym, J. Whangbo *et al.*, 2003 Identification of genes that regulate a left-right asymmetric neuronal migration in *Caenorhabditis elegans*. Genetics 164: 1355–1367.

Collins, C. A., Y. P. Wairkar, S. L. Johnson, and A. Diantonio, 2006 Highwire restrains synaptic growth by attenuating a MAP kinase signal. Neuron 51: 57–69.

D'Souza, J., M. Hendricks, S. Le Guyader, S. Subburaju, B. Grunewald *et al.*, 2005 Formation of the retinotectal projection requires Esrom, an ortholog of PAM (protein associated with Myc). Development 132: 247–256.

Grill, B., W. V. Bienvenut, H. M. Brown, B. D. Ackley, M. Quadroni *et al.*, 2007 C. elegans RPM-1 regulates axon termination and synaptogenesis through the Rab GEF GLO-4 and the Rab GTPase GLO-1. Neuron 55: 587–601.

Hallam, S. J., and Y. Jin, 1998 lin-14 regulates the timing of synaptic remodelling in Caenorhabditis elegans. Nature 395: 78–82.

Hammarlund, M., P. Nix, L. Hauth, E. M. Jorgensen, and M. Bastiani, 2009 Axon regeneration requires a conserved MAP kinase pathway. Science 323: 802–806.

Han, S., R. M. Witt, T. M. Santos, C. Polizzano, B. L. Sabatini *et al.*, 2008 Pam (Protein associated with Myc) functions as an E3

ubiquitin ligase and regulates TSC/mTOR signaling. Cell. Signal. 20: 1084–1091.
Hanada, M., J. Ninomiya-Tsuji, K. Komaki, M. Ohnishi, K. Katsura *et al.*, 2001 Regulation of the TAK1 signaling pathway by protein phosphatase 2C. J. Biol. Chem. 276: 5753–5759.
Jackson, M. D., C. C. Fjeld, and J. M. Denu, 2003 Probing the function of conserved residues in the serine/threonine phosphatase PP2Calpha. Biochemistry 42: 8513–8521.
Jacoby, T., H. Flanagan, A. Faykin, A. G. Seto, C. Mattison *et al.*, 1997 Two protein-tyrosine phosphatases inactivate the osmotic stress response pathway in yeast by targeting the mitogen-activated protein kinase, Hog1. J. Biol. Chem. 272: 17749–17755.
Ji, R. R., R. W. t. Gereau, M. Malcangio, and G. R. Strichartz, 2009 MAP kinase and pain. Brain Res. Brain Res. Rev. 60: 135–148.
Lewcock, J. W., N. Genoud, K. Lettieri, and S. L. Pfaff, 2007 The ubiquitin ligase Phr1 regulates axon outgrowth through modulation of microtubule dynamics. Neuron 56: 604–620.
Li, D., F. Wang, M. Lai, Y. Chen, and J. F. Zhang, 2005 A protein phosphatase 2calpha-Ca2+ channel complex for dephosphorylation of neuronal Ca2+ channels phosphorylated by protein kinase C. J. Neurosci. 25: 1914–1923.
Li, H., G. Kulkarni, and W. G. Wadsworth, 2008 RPM-1, a Caenorhabditis elegans protein that functions in presynaptic differentiation, negatively regulates axon outgrowth by controlling SAX-3/robo and UNC-5/UNC5 activity. J. Neurosci. 28: 3595–3603.
Liao, E. H., W. Hung, B. Abrams, and M. Zhen, 2004 An SCF-like ubiquitin ligase complex that controls presynaptic differentiation. Nature 430: 345–350.
Lu, G., and Y. Wang, 2008 Functional diversity of mammalian type 2C protein phosphatase isoforms: new tales from an old family. Clin. Exp. Pharmacol. Physiol. 35: 107–112.
Maeda, T., S. M. Wurgler-Murphy, and H. Saito, 1994 A two-component system that regulates an osmosensing MAP kinase cascade in yeast. Nature 369: 242–245.
Mello, C. C., J. M. Kramer, D. Stinchcomb, and V. Ambros, 1991 Efficient gene transfer in C.elegans: extrachromosomal maintenance and integration of transforming sequences. EMBO J. 10: 3959–3970.
Murthy, V., S. Han, R. L. Beauchamp, N. Smith, L. A. Haddad *et al.*, 2004 Pam and its ortholog highwire interact with and may negatively regulate the TSC1.TSC2 complex. J. Biol. Chem. 279: 1351–1358.
Nakata, K., B. Abrams, B. Grill, A. Goncharov, X. Huang *et al.*, 2005 Regulation of a DLK-1 and p38 MAP kinase pathway by the ubiquitin ligase RPM-1 is required for presynaptic development. Cell 120: 407–420.
Nguyen, A. N., and K. Shiozaki, 1999 Heat-shock-induced activation of stress MAP kinase is regulated by threonine- and tyrosine-specific phosphatases. Genes Dev. 13: 1653–1663.
Nix, P., N. Hisamoto, K. Matsumoto, and M. Bastiani, 2011 Axon regeneration requires coordinate activation of p38 and JNK MAPK pathways. Proc. Natl. Acad. Sci. USA 108: 10738–10743.
Park, E. C., D. R. Glodowski, and C. Rongo, 2009 The ubiquitin ligase RPM-1 and the p38 MAPK PMK-3 regulate AMPA receptor trafficking. PLoS ONE 4: e4284.
Po, M. D., C. Hwang, and M. Zhen, 2010 PHRs: bridging axon guidance, outgrowth and synapse development. Curr. Opin. Neurobiol. 20: 100–107.
Saiga, T., T. Fukuda, M. Matsumoto, H. Tada, H. J. Okano *et al.*, 2009 Fbxo45 forms a novel ubiquitin ligase complex and is required for neuronal development. Mol. Cell. Biol. 29: 3529–3543.
Saito, H., and K. Tatebayashi, 2004 Regulation of the osmoregulatory HOG MAPK cascade in yeast. J. Biochem. 136: 267–272.
Samuels, I. S., S. C. Saitta, and G. E. Landreth, 2009 MAP'ing CNS development and cognition: an ERKsome process. Neuron 61: 160–167.
Schaefer, A. M., G. D. Hadwiger, and M. L. Nonet, 2000 rpm-1, a conserved neuronal gene that regulates targeting and synaptogenesis in C. elegans. Neuron 26: 345–356.
Shi, Y., 2009 Serine/threonine phosphatases: mechanism through structure. Cell 139: 468–484.
Stern, A., E. Privman, M. Rasis, S. Lavi, and T. Pupko, 2007 Evolution of the metazoan protein phosphatase 2C superfamily. J. Mol. Evol. 64: 61–70.
Tada, H., H. J. Okano, H. Takagi, S. Shibata, I. Yao *et al.*, 2009 Fbxo45, a novel ubiquitin ligase, regulates synaptic activity. J. Biol. Chem. 285: 3840–3849.
Takekawa, M., T. Maeda, and H. Saito, 1998 Protein phosphatase 2Calpha inhibits the human stress-responsive p38 and JNK MAPK pathways. EMBO J. 17: 4744–4752.
Trujillo, G., K. Nakata, D. Yan, I. N. Maruyama, and Y. Jin, 2010 A ubiquitin E2 variant protein acts in axon termination and synaptogenesis in *Caenorhabditis elegans*. Genetics 186: 135–145.
Wan, H. I., A. DiAntonio, R. D. Fetter, K. Bergstrom, R. Strauss *et al.*, 2000 Highwire regulates synaptic growth in Drosophila. Neuron 26: 313–329.
Wu, C., R. W. Daniels, and A. DiAntonio, 2007 DFsn collaborates with Highwire to down-regulate the Wallenda/DLK kinase and restrain synaptic terminal growth. Neural Dev. 2: 16.
Yan, D., Z. Wu, A. D. Chisholm, and Y. Jin, 2009 The DLK-1 kinase promotes mRNA stability and local translation in C. elegans synapses and axon regeneration. Cell 138: 1005–1018.
Zhen, M., X. Huang, B. Bamber, and Y. Jin, 2000 Regulation of presynaptic terminal organization by C. elegans RPM-1, a putative guanine nucleotide exchanger with a RING-H2 finger domain. Neuron 26: 331–343.

Communicating editor: M. Nonet